Enolization in Radical Cations of *o*-Methylacetophenone and Related Species under Cryogenic Conditions

Andrzej Marcinek,[a] **Jacek Michalak,**[a,b] **Jacek Rogowski,**[a] **Weilin Tang,**[b] **Thomas Bally***[,b] **and Jerzy Gębicki***[,a]
[a] *Institute of Applied Radiation Chemistry, Techinical University, Zwirki 36, 90–924 Lodz, Poland*
[b] *Institute of Physical Chemistry, University of Fribourg, Pèrolles, CH-1700 Fribourg, Switzerland*

Upon radiolytic ionization of *o*-methylacetophenone in low temperature matrices, the radical cation of the corresponding enol is formed. The kinetics of this process indicate a significant contribution of quantum-mechanical tunnelling in the hydrogen atom transfer. The same species is also formed by ionizing 1-methyl-1,2-dihydrobenzocyclobutenol but the composition of the rotameric mixture of enol radical cations is different in this case. Analogous experiments with 5,8-dimethyl-1-tetralone demonstrate that enol radical cations are stable in their *Z*-conformation under cryogenic conditions in contrast to the corresponding neutrals.

Aromatic carbonyl compounds bearing an alkyl group in the *ortho*-position may undergo hydrogen atom transfer upon photoexcitation to form the corresponding conjugated enols.[1] The mechanism of this reaction is well known and involves formation of a biradical regarded as the common precursor for two different enols, *Z* and *E*. These enols, having quite similar spectroscopic properties, are very different in their kinetic behaviour. Only the *E*-enol could be stabilized in non-polar solvents under cryogenic conditions.[2] It is believed that under such conditions the *Z*-enol is generated, but re-ketonizes back, most probably with the involvement of quantum-mechanical tunnelling.

Alternatively, transient enols can be formed by thermolysis of corresponding benzocyclobutenols.[1a] This is shown in Scheme 1, using *o*-methylacetophenone (**1**) and 1-methyl-1,2-dihydrobenzocyclobuten-1-ol (**2**) as an example.

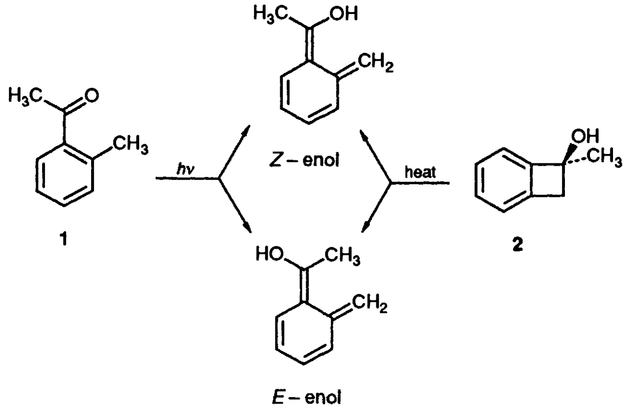

Scheme 1

We have recently shown that upon radiolytic ionization various *ortho*-substituted aromatic carbonyl compounds in low-temperature matrices undergo spontaneous hydrogen atom transfer to yield radical cations with *o*-quinoid structures.[3] This paper presents a more detailed account of our findings with regard to the methyl substituted compounds, **1** and **2**, as well as the related model system, 5,8-dimethyl-1-tetralone (**3**). We will address the questions concerning spectroscopic characterization of enol radical cations as well as the kinetics of the enolization processes.

Chemical structures of the compounds studied, including some deuteriated derivatives, are specified below.

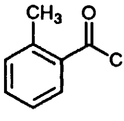
1

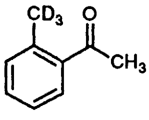
[$^2H_3$]-**1**

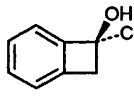
2

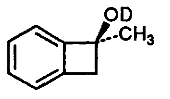
[$^2H_1$]-**2**

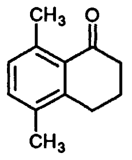
3

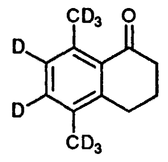
[$^2H_8$]-**3**

Experimental

Materials.—*o*-Methylacetophenone (**1**) (Aldrich) was used without further purification. Deuterium-labelled *o*-methylacetophenone, ([$^2H_3$]-**1**) (isotopic purity, 99.8%) was prepared according to modified procedures described for similar compounds[4] and the purified final product was characterized by IR, NMR and MS spectra. 1-Methyl-1,2-dihydrobenzocyclobuten-1-ol (**2**) was prepared from benzocyclobuten-1-one[5] and purified by silica gel column chromatography. The corresponding derivative deuteriated on the hydroxy group, [$^2H_1$]-**2**, was obtained by isotope exchange in D_2O. 5,8-Dimethyl-1-tetralone (**3**) and its deuteriated derivative [$^2H_8$]-**3** were synthesized from *p*-xylene and [$^2H_{10}$]-*p*-xylene respectively, using a procedure adopted from that described for 2,5,8-trimethyl-1-tetralone.[6]

Techniques.—The method of preparation of radical cations in argon matrices has been described previously.[7] Briefly, a 1:1 mixture of the precursor and methylene dichloride is mixed with a 10^3-fold excess of Ar and *ca.* 2 mmol of this mixture is deposited on a CsI window held at 20 K. In the case of **2** and **3**, whose vapour pressure is too low to permit pre-mixing with Ar at room temperature, the precursor is placed in a thermostatted U-tube just in front of the inlet valve and a 1:1000 mixture of CH_2Cl_2–Ar is slowly passed over the substrate before spray-on. In these experiments, **2** was held at −5 °C and **3** at +8 °C to achieve optimal concentrations in the matrices. After the sample had been cooled to the lowest temperature attainable by closed-cycle cryostat (~12 K) it was exposed to X-rays.

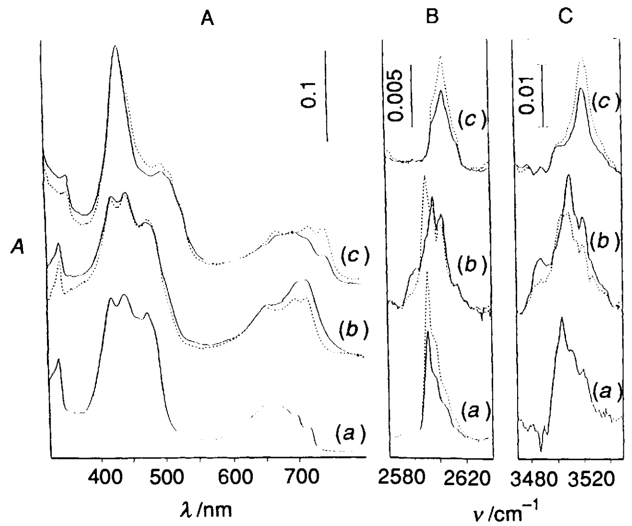

Fig. 1 UV–VIS (A) and IR (B, C) spectra of enol radical cations (solid lines, neutral subtracted) generated in argon matrices from *o*-methylacetophenone (*a*), 1-methylbenzocyclobutenol (*b*) and 5,8-dimethyl-1-tetralone (*c*). Traces in part B obtained for properly deuteriated derivatives. Spectral changes induced by photolysis at 700 nm (30 min) (dotted lines).

Description of the pulse radiolysis system and procedure for the steady-state and time-resolved radiolytic measurements in hydrocarbon matrices are given elsewhere.[8] For these measurements at temperatures below 77 K a liquid helium-cooled cryostat (Oxford Instruments) was used.

Results and Discussion

Characterization of Enol Radical Cations in Argon Matrices.—The results of the experiments in argon matrices are summarized in Fig. 1. The left panel (Fig. 1A) shows the UV–VIS spectra observed after X-irradiation of **1**, **2** and **3**, respectively, and the changes induced by subsequent photolysis with the visible light (dashed lines). All the spectra can be interpreted in terms of electronic transitions of the four lowest excited states of the corresponding *o*-quinoid enol radical cations as shown below.

o-Xylylene (**4**) radical cation, which may serve as a model for the *o*-quinoid structure, shows similar bands observed at 860, 525 and 440 nm.[9] Open shell PPP-CI calculations[10a] on **4**$^{\cdot+}$ predict transitions at 998 (ε = 1500), 508 (2800) and 456 nm (4400) in addition to another band at 370 nm (2400).[10b] Thus, PPP-CI appears to underestimate the energy of the first excited state of **4**$^{\cdot+}$, which corresponds largely to HOMO ⟶ LUMO excitation, by *ca.* 0.2 eV while the next two states are predicted to within 0.1 eV.*

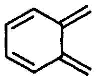

4

Encouraged by the success of this simple model we applied it to the present case of **1**$^{\cdot+}$.† Owing to the absence of the C_2 symmetry element, configurational mixing is more extensive in this compound than in **4**$^{\cdot+}$ but inspection of the CI eigen vectors shows that the character of the first few excited states is essentially preserved. Optical transitions of the enol form of **1**$^{\cdot+}$ are predicted at 788 (ε = 1300), 460 (1300), 447 (4700) and 355 nm (2000) which compare favourably with the observed bands at 700, 470, 430 and 345 nm. Again, the first excitation energy is underestimated by 0.2 eV while the next three are predicted more accurately. More importantly, the shifts introduced by the OH group are reproduced correctly and it is clear that the optical spectra in Fig. 1 do indeed correspond to radical cations with the *o*-quinoid structure.

The two right-hand panels (B and C in Fig. 1) show the spectral changes after X-irradiation and subsequent photolysis in selected sections of the IR spectra. In all cases we do find new absorptions around 3500 or 2600 cm^{-1} (deuteriated compounds), respectively, which arise at the expense of the bands of the keto precursors. Since we know from the related examples that the corresponding neutral enols absorb at significantly higher energy (around 3650 and 2700 cm^{-1}, respectively, for the OH and OD stretches[2,11]) we conclude that IR bands shown in Fig. 1 are also due to enol radical cations with the *o*-quinoid structure. A slight weakening of the OH (OD) bands in enol radical cations as compared with the neutral enols is not unexpected, since the OH (OD) groups are adjacent to the electron deficient π systems.

With the exception of **1**, the IR bands change in shape upon irradiation with visible light in concert with the UV–VIS bands. In [$^2H_3$]-**1** and [$^2H_8$]-**3** the OD bands increase which indicates that additional enol radical cations are formed upon photoexcitation. This is in agreement with the pulse radiolysis experiments which indicate much slower enolization processes in deuteriated derivatives (*cf.* below). Interestingly, both UV–VIS and IR bands of **1**$^{\cdot+}$ have a different shape depending on the mode of formation (from **1** or from **2**). Indeed, it would be surprising if this were not the case because there is no reason why the distribution among the four possible rotamers (*E*′, *E*″, *Z*′ and *Z*″) of enol radical cations of **1** should be identical in both cases.

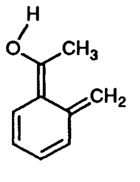

E′

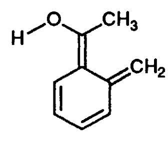

E″

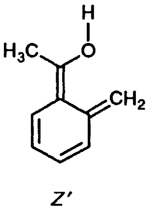

Z′

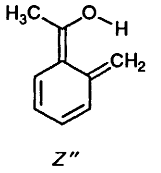

Z″

Apparently it is possible to induce some interconversion among the four rotamers of **1**$^{\cdot+}$ by further visible irradiation (*cf.* dotted lines in Fig. 1). Thus, it becomes evident that a rotamer with an IR peak at 3490 cm^{-1} (2580 cm^{-1} for OD) which is only formed from **2** can be partially transformed into the major component originating from **1**, which absorbs at 3502 cm^{-1}

---

* It is interesting to note that the PPP-CI predictions are considerably more accurate than those obtained by the more sophisticated all-valence procedure which are off by *ca.* 0.5 eV for the first and 0.3 eV for the next two excited states.[9]

† For the OH oxygen we took the parameters proposed by Wirz:[10c] $Z^c = 2$, $I_\mu = 21.48$ eV relative to carbon, $\gamma_{\mu\mu} = 22.9$ eV. Owing to the shorter CO bond β_{CO} was increased relative to β_{CC} by 30%.

(2590 cm^{-1}). The fact that the distribution of enol rotamers arising from **1** is insensitive to visible photolysis seems to indicate a photostationary equilibrium between rotamers which cannot be changed under the conditions of irradiation employed in our experiments. Unfortunately, in the present situation we are not in a position to assign different components of the complex IR bands to individual rotamers of enol radical cation, as is possible in the related case of *o*-methylbenzaldehyde.[11]

Kinetics of the Enolization Process.—The spectra of enol radical cations generated by γ-rays from **1** and **3** in frozen organic glasses at 77 K were very much similar to those presented in Fig. 1A. However, the yield of enol radical cations was found to be lower for deuteriated derivatives which suggested a strong isotope effect for the hydrogen transfer reaction. Thus we decided to study the kinetics of this reaction by low-temperature pulse radiolysis.[8] The transient UV–VIS spectra similar to those obtained in the steady-state experiments were observed to grow with time.

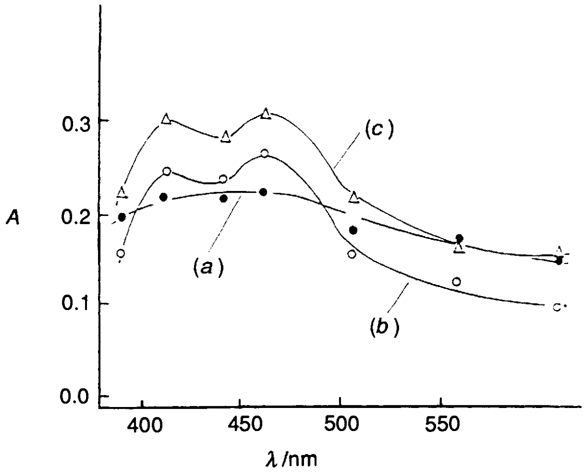

Fig. 2 Transient absorption spectra for solutions of deuteriated [$^2H_3$]-*o*-methylacetophenone [(*a*) and (*b*)] and *o*-methyl-acetophenone (*c*) at 83 K obtained 90 ms [(*a*) and (*c*)] and 9 s (*b*) after the 2 μs electron pulse delivering a dose of 500 Gy. The sample contained the substrate (0.02 mol cm^{-3}) and butyl chloride (1 mol dm^{-3}) in methylcyclohexane.

As an example, the time-resolved spectra for **1** and [$^2H_3$]-**1** are presented in Fig. 2. It is clearly seen in the case of [$^2H_3$]-**1** that at early stages of observation practically no absorption due to the enol radical cation [curve (*a*)] was seen and in the time-scale of seconds characteristic absorption was built up [curve (*b*)]. The keto-form of the radical cation generated from **1**, as compared to the non-enolizable radical cations of *meta* or *para* methyl-substituted acetophenones, is represented by a very weak absorption (ε ~ 150) in this region which practically did not disturb the observation of absorption growth due to the enolization process in $\mathbf{1}^{\cdot+}$. It is also evident that the rate of enolization for the deuteriated sample was much lower. The spectrum of $\mathbf{1}^{\cdot+}$ detected 90 ms after the electron pulse [curve (*c*) shows the characteristic absorptions of the enol radical cation whereas no such enol absorptions were detected for the deuteriated sample under similar conditions [curve (*a*)].

The kinetics of enolization can be followed by monitoring the absorption growth due to the enol radical cation with time. As a unimolecular reaction, the enolization should, in principle, fit first-order kinetics. However, the experimental data do not follow such kinetics, as is shown in Fig. 3 (curves A′ and A″), which suggests a perturbation introduced by a rigid matrix environment on the structure of the reacting molecules. Similar effects have been observed for unimolecular conformation-dependent charge delocalization in the diamine radical cations.[12]

A better kinetic description of the process can be achieved by applying a model of dispersive kinetics with the time-dependent rate constant in the form of eqn. (1), where the coefficient

$$k(t) = Bt^{\alpha-1} \qquad (1)$$

$0 \leqslant \alpha < 1$ measures the reactivity dispersion.[13] The first-order kinetic eqn. (2) with the time dependent rate coefficient [eqn.

$$-\frac{dc}{dt} = k(t)c \qquad (2)$$

(1)] on integration gives the relation (3) which fits our experimental results well (Fig. 3, curves B′ and B″).

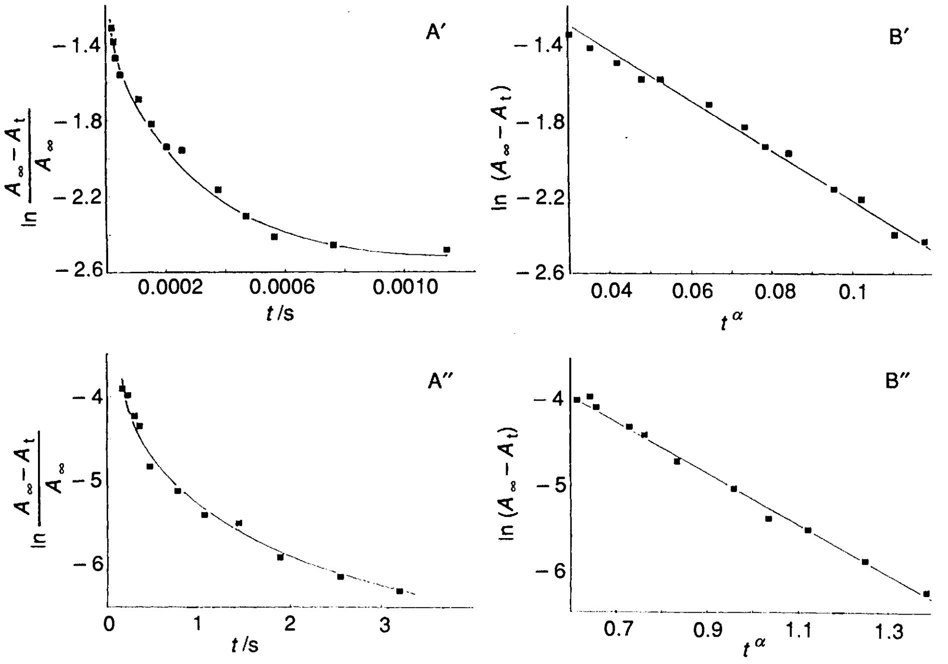

Fig. 3 Experimental data for the absorption growth of *o*-methylacetophenone radical cation at 90 K (A′ and B′) and 50 K (A″ and B″) presented in coordinates suitable for classical (A) and dispersive (B) kinetics. Wavelength monitored: 460 nm.

Table 1 Parameters of dispersive kinetics and values of kinetic isotope effects for enolization of the radical cations of *o*-methylacetophenone (**1**) and deuteriated [$^2H_3$]-*o*-methylacetophenone in methylcyclohexane glass at various temperatures

Sample	T/K	α	τ_0/s	$\langle E\rangle$/kJ mol^{-1}	σ^2/kJ^2 mol^{-2}	k_H/k_D [a]
1	93	0.33	0.0022 ± 0.0002	12.16 ± 0.01	4.05	
	90	0.30	0.0070 ± 0.0002	12.50 ± 0.01	5.00	
	88	0.33	0.0116 ± 0.0001	12.72 ± 0.01	3.62	
	83	0.30	0.0158 ± 0.0005	12.09 ± 0.01	4.26	
	50	0.29	0.0359 ± 0.0030	7.60 ± 0.01	1.70	
	30	0.27	0.0368 ± 0.0040	4.53 ± 0.01	0.75	
[$^2H_3$]-**1**	83	0.33	0.62 ± 0.01	12.73 ± 0.01	3.63	39
	77	0.28	4.16 ± 0.30	14.69 ± 0.01	4.54	(120)
	50	0.30	120 ± 10	11.02 ± 0.01	1.55	3340

[a] $k_H/k_D = (\tau_0)_D/(\tau_0)_H$.

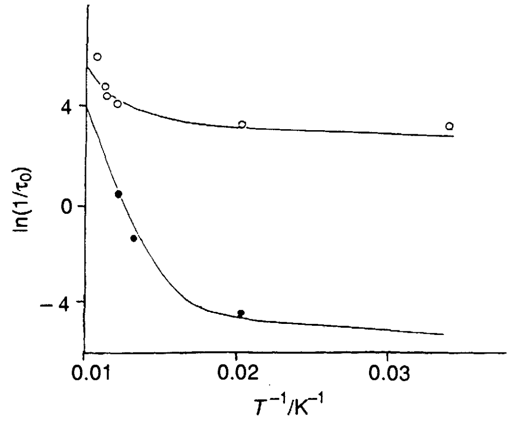

Fig. 4 Rate constants of the enolization process in radical cations of *o*-methylacetophenone (○) and deuteriated [$^2H_3$]-*o*-methylacetophenone (●) presented in the Arrhenius coordinates. The lines represent the best fit using the Bell model of quantum-mechanical tunnelling (see text).

$$\ln\frac{c}{c_0} = -\frac{Bt^\alpha}{\alpha} = -(t/\tau_0)^\alpha \qquad (3)$$

Phenomenologically, the decrease in the rate coefficient $k(t)$ with time according to eqn. (1) implies[13] that the activation energy for the reaction increases as shown in eqn. (4), where

$$E = E_0 + (1 - \alpha)\,RT\ln(t/\tau_0) \qquad (4)$$

$\tau_0 = (\alpha/B)^{1/\alpha}$ for the first-order reaction. This makes it possible to obtain the distribution function for activation energy $F(E)$ from the reaction progress: $F(t) = 1 - c/c_0$. The first moments of the activation energy distribution,[13] *i.e.* the mean value of activation energy $\langle E\rangle$ [eqn. (5)] and the dispersion characterizing the width of activation energy distributions [eqn. (6)] are given in Table 1 together with the kinetic parameters used in the

$$\langle E\rangle = E_0 - 0.577(1 - \alpha)RT/\alpha \qquad (5)$$

$$\sigma^2 = \frac{\pi^2}{6}\,[(1 - \alpha)RT/\alpha]^2 \qquad (6)$$

fitting procedure. For **1** and [$^2H_3$]-**1** these parameters were calculated assuming that the absorption observed just after the pulse corresponds to the reaction progress during the time of the pulse duration. The parameter α which represents the dispersion of reactivities was found to be almost temperature-independent (Table 1) and seems to characterize a particular system of substrate and matrix. The distribution of reactivities can be interpreted in terms of matrix-induced conformational disorder characterizing different geometrical orientations of the carbonyl and methyl groups. Changes in the distance between the oxygen and carbon atoms introduced by such a disorder will affect the rate of the hydrogen atom transfer.

The rate constants $k = 1/\tau_0$ from Table 1 are presented in the form of the Arrhenius plot in Fig. 4. The strong curvature of the Arrhenius plot indicates participation of quantum-mechanical tunnelling in the hydrogen atom transfer.[14] To verify the operation of such a mechanism in the enolization processes we introduced a tunnelling correction factor Q in the rate constant expression [eqn. (7)], which is, among other variables,

$$k = QAe^{-E/RT} \qquad (7)$$

a function of temperature (A and E are the normal Arrhenius parameters). To reproduce the temperature dependence we have to adopt a model for the tunnelling calculations. The simplest one is that developed by Bell involving a parabolic barrier of width $2a$ and heights E.[14a] With this barrier the expression for Q is given by eqn. (8), where $\alpha = E/RT$ and $\beta =$

$$Q = \frac{e^\alpha}{\beta - \alpha}(\beta e^{-\alpha} - \alpha e^{-\beta}) \qquad (8)$$

$2\pi^2 a(2mE)^{\frac{1}{2}}/h$. Assuming log $A = 10$ and taking the mass of hydrogen or deuterium atoms as the mass of the tunnelling particles the best fit (lines in Fig. 4) of this model to the experimental points was obtained for $E = 16.8$ kJ mol^{-1} and $2a = 1.44$ Å. Owing to the crudeness of the model, the obtained values for parameters E and $2a$ carry some uncertainty; nevertheless, both these values are quite reasonable. A good correlation of experimental data both for the protiated and the deuteriated molecules with the Bell model seem to indicate clearly the operation of quantum-mechanical tunnelling in the enolization process of *o*-methylacetophenone radical cation.

Similar conclusions can also be drawn from the kinetic studies of the enolization process in the radical cation generated from 5,8-dimethyl-1-tetralone (**3**). A substantial kinetic isotope effect k_H/k_D (210 at 83 K and 3460 at 77 K) was detected in this case. The best fit of experimental data for **3** and [$^2H_8$]-**3** with the Bell model was obtained for $E = 20.1$ kJ mol^{-1} and $2a = 1.40$ Å.

Observation of a large kinetic isotope effect on low-temperature tautomerization of neutral enol generated photochemically from **1** was reported[15] and similarly interpreted in terms of a significant contribution of tunnelling in the hydrogen atom transfer.

Acknowledgements

This work was supported by the Polish Committee for Scientific

Research (grant no. 2 1315 91 01) and by the Swiss National Science Foundation (grant no. 20-28842.90). We thank Drs. R. Kaminski and J. Adamus for the preparation of deuteriated *o*-methylacetophenone.

References

1 (*a*) P. G. Sammes, *Tetrahedron*, 1976, **32**, 405; (*b*) R. Haag, J. Wirz and P. J. Wagner, *Helv. Chim. Acta*, 1977, **60**, 2595; (*c*) J. C. Scaiano, *Acc. Chem. Res.*, 1982, **15**, 252; (*d*) P. J. Wagner, *Acc. Chem. Res.*, 1989, **22**, 83; (*e*) A. C. Weedon, in *The Chemistry of Enols*, ed. Z. Rappaport, Wiley, Chichester, 1990, p. 591.

2 (*a*) J. Gębicki and A. Krantz, *J. Chem. Soc., Perkin Trans. 2*, 1984, 1623; (*b*) J. Gębicki, S. Kuberski and R. Kaminski, *J. Chem. Soc., Perkin Trans. 2*, 1990, 765.

3 J. Gębicki, A. Marcinek, J. Michalak, J. Rogowski, T. Bally and W. Tang, *J. Mol. Struct.*, in the press.

4 A. I. Vogel, *Textbook of Practical Organic Chemistry*, Longman Group, London, 1978.

5 B. J. Arnold, P. G. Sammes and T. W. Wallace, *J. Chem. Soc., Perkin Trans. 1*, (*a*) 1974, 409; (*b*) 1974, 415.

6 E. J. Eisenbraun, C. W. Hinman, J. M. Springer, J. W. Burnham, T. S. Chou, D. W. Flanagan and M. C. Hamming, *J. Org. Chem.*, 1971, **36**, 2480.

7 T. Bally, in *Radical Ionic Systems*, eds. A. Lund and M. Shiotani, Kluwer, Dordrecht, 1991, p. 3.

8 (*a*) S. Karolczak, K. Hodyr, R. Lubis and J. Kroh, *J. Radioanal. Nucl. Chem.*, 1986, **101**, 177; (*b*) J. Gębicki, A. Marcinek and J. Rogowski, *Radiat. Phys. Chem.*, 1992, **39**, 41.

9 K. Kesper, N. Münzel, W. Pietzuch, H. Specht and A. Schweig, *J. Mol. Struct. (Theochem.)*, 1989, **200**, 375.

10 (*a*) P. Carsky and R. Zahradnik, *Top. Curr. Chem.*, 1973, **43**, 1; (*b*) T. Bally, unpublished work; (*c*) E. Rommel and J. Wirz, *Helv. Chim. Acta*, 1977, **60**, 38.

11 T. Bally and W. Tang, unpublished work.

12 A. Marcinek, J. Gębicki and A. Plonka, *J. Phys. Org. Chem.*, 1990, **3**, 757.

13 (*a*) A. Plonka, *Time-Dependent Reactivity of Species in Condensed Media, Lecture Notes in Chemistry*, vol. 40, Springer, Heidelberg, 1986; (*b*) A. Plonka, *Annu. Rep. Prog. Chem., Sect. C, Phys. Chem.*, 1989, **85**, 47; (*c*) A. Plonka, *Prog. React. Kinet.*, 1991, **16**, 157.

14 (*a*) E. F. Caldin, *Chem. Rev.*, 1969, **69**, 135; (*b*) M. D. Harmony, *Chem. Soc. Rev.*, 1972, **1**, 211; (*c*) V. I. Goldanskii, *Annu. Rev. Phys. Chem.*, 1976, **27**, 85; (*d*) V. I. Goldanskii, *Nature*, 1979, **279**, 109.

15 K. H. Grellmann, H. Weller and E. Tauer, *Chem. Phys. Lett.*, 1983, **95**, 195.

Paper 2/02041F
Received 22nd *April* 1992
Accepted 17th *May* 1992